Non-Perturbative Studies of Color Confinement

Attilio Cucchieri

http://lattice.ifsc.usp.br/

Instituto de Física de São Carlos

Universidade de São Paulo

Abstract

After more than forty years from the formulation of Quantum Chromodynamics (QCD), we are still lacking a complete understanding of one of the main properties of the strong force: color confinement. The discretized version of QCD (Lattice QCD), besides allowing precise calculations that can be compared to experimental data, permits a quantitative testing of theoretical ideas that can give us useful insights for the explanation of the confinement phenomenon in QCD. In particular, Lattice QCD simulations provide accurate results for the infrared (non-perturbative) behavior of propagators and vertices of the theory (in a given gauge). These outcomes can be used as input in analytic works and help us gain a conceptual understanding of color confinement. The talk will address some of the theoretical and computational issues that are involved in the study of the infrared behavior of Green's functions in non-Abelian Yang-Mills theories.

Color Confinement

Millennium Prize Problems by the Clay Mathematics Institute (US$1,000,000): Yang-Mills Existence and Mass Gap: Prove that for any compact simple gauge group G, a non-trivial quantum Yang-Mills theory exists on $\mathbb{R}^4$ and has a mass gap $\Delta > 0$.

Lattice simulations can solve QCD exactly (in discretized Euclidean space-time), allowing quantitative predictions for the physics of hadrons. But they can also help reveal the principles behind a central phenomenon of QCD: confinement. In fact, we can try to understand the QCD vacuum (the “battle for nonperturbative QCD”, E.V. Shuryak, *The QCD vacuum, hadrons and the superdense matter*) by using inputs from lattice simulations and by testing numerically the approximations introduced in analytic approaches (Dyson-Schwinger equations, Bethe-Salpeter equations, Pomeron dynamics, QCD-inspired models, etc).

Lattice QCD

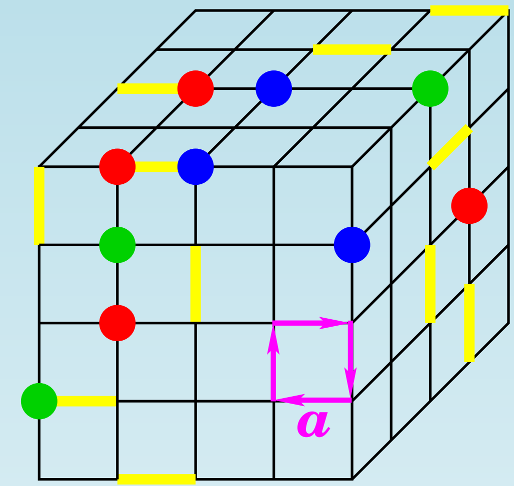

Three ingredients:

1. Quantization by path integrals $\Rightarrow$ sum over configurations with "weights" $e^{i\,S/\hbar}$
2. Euclidean formulation (analytic continuation to imaginary time) $\Rightarrow$ weight becomes $e^{-S/\hbar}$
3. Discrete space-time $\Rightarrow$ UV cut at momenta $p \lesssim 1/a$ $\Rightarrow$ regularization

Also: finite-size lattices $\Rightarrow$ IR cut for small momenta $p \approx 1/L$

The Wilson action (1974)

$$S \;=\; -\frac{\beta}{3}\sum_{\square}\mathrm{Re}\,\mathrm{Tr}\,U_{\square}\;, \quad U_\mu(x) \;\equiv\; e^{i g_0\, a\, A^b_\mu(x) T_b}\;, \quad \beta \;=\; 6/{g_0}^2$$

- written in terms of oriented plaquettes formed by the link variables $U_\mu(x)$, which are group elements;
- gauge transformations: $U_\mu(x) \to \omega(x)\, U_\mu(x)\, \omega^\dagger(x + a\, e_\mu)$, where $\omega(x) \in SU(3)$ $\Rightarrow$ closed loops are gauge-invariant;
- reduces to the usual action for $a \to 0$.

LQCD: a Grand Challenge Problem

Numerical aspects:

- Application of statistical-mechanics techniques — such as Monte Carlo simulation, study of critical phenomena — to quantum field theories.
- Data analysis resembles experimental physics, need for large computer resources ⇒ lattice-QCD collaborations.

Run-time acceptability variation by scientific culture:

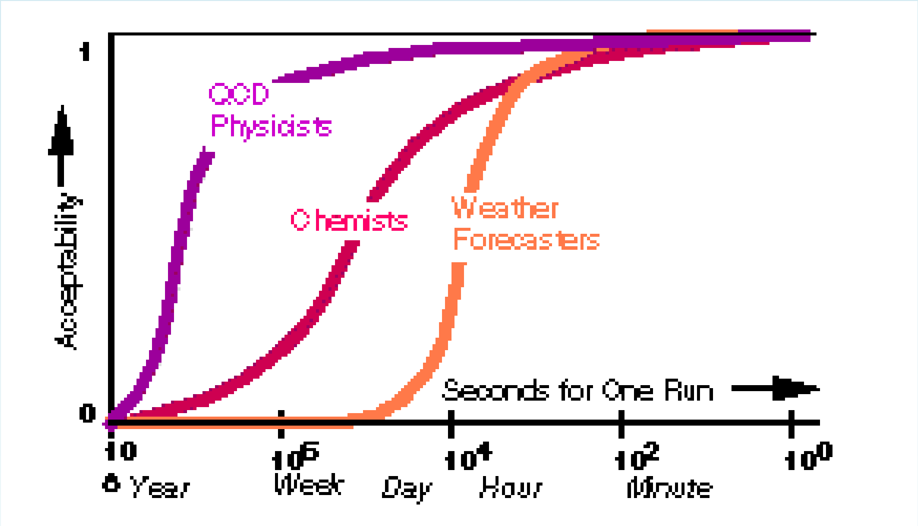

"QCD physicists have an extraordinary tolerance for execution times that take a significant fraction of a human lifetime"

Spectroscopy and Strong Coupling

High-precision results from Lattice QCD simulations

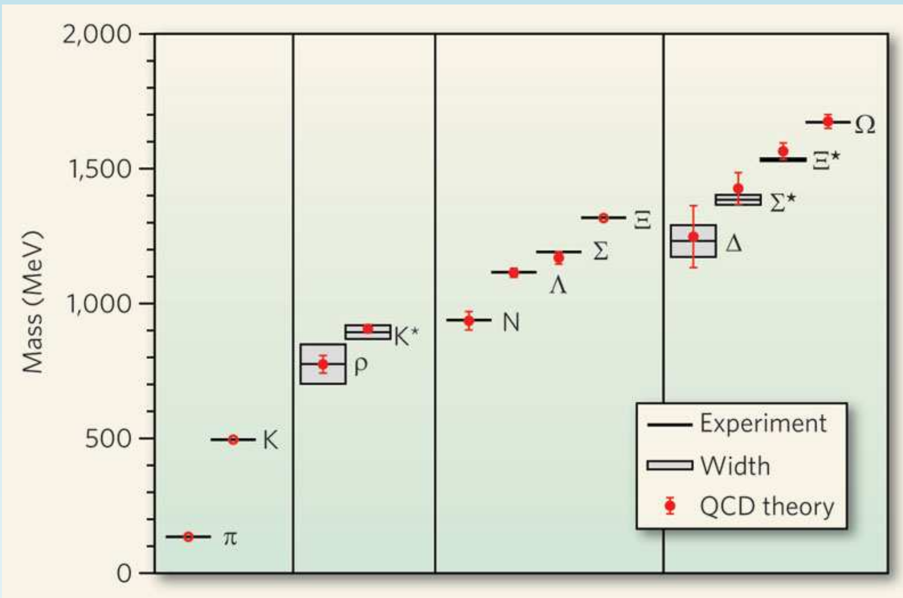

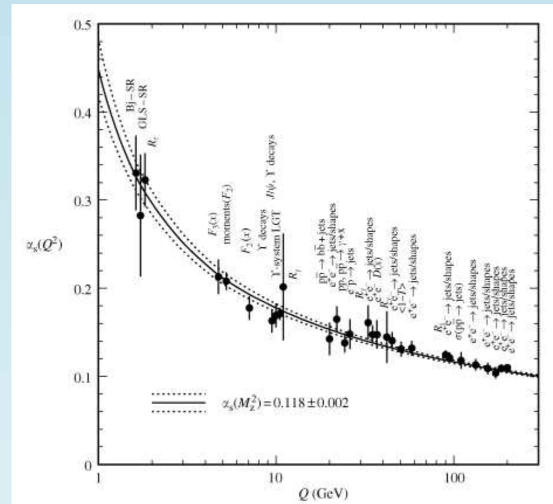

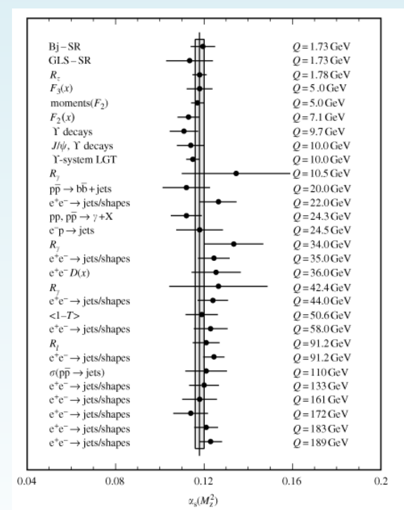

Numerical determination of hadron masses (above) and of the strong coupling constant $\alpha_s(\overline{\mu})$ (left).

Lattice QCD at the IFSC–USP

The only LQCD group (A.C. & T. Mendes) in South America.

1. Study of qualitative aspects of QCD: infrared behavior of propagators and vertices, related to color confinement and to color deconfinement (at high temperature).
2. Development of methods: determination of the strong coupling constant $\alpha_s(p)$ to be applied to the full QCD case, lattice implementation of different analytic approaches (linear covariant gauge, background gauge).
3. Development of algorithms: gauge fixing, global minimization, matrix inversion, evaluation of eigenvalues.

Pathways to Confinement

- How does linearly rising potential (seen in lattice QCD) come about?
- Theories of quark confinement include:
  dual superconductivity (electric flux tube connecting magnetic monopoles), condensation of center vortices, etc.
- Proposal by Mandelstam (1979) linking linear potential to infrared behavior of gluon propagator as $1/p^4$.
- Green's functions carry all information of a QFT's physical and mathematical structure.
- Confinement given by behavior at large distances (small momenta) $\Rightarrow$ nonperturbative study of IR propagators and vertices $\longrightarrow$ it requires very large lattice volumes.
- Gribov-Zwanziger confinement scenario based on suppressed gluon propagator and enhanced ghost propagator in the IR.

Lattice Landau Gauge

The lattice Landau gauge is imposed by minimizing the functional

$$S[U;\omega] \,=\, -\sum_{x,\mu} Tr\, U_\mu^\omega(x) \ ,$$

where $\omega(x) \in SU(N)$ and $U_\mu^\omega(x) \,=\, \omega(x)\, U_\mu(x)\, \omega^\dagger(x + a\, e_\mu)$ is the lattice gauge transformation.

By considering the relations $U_\mu(x) \,=\, e^{i\, a\, g_0\, A_\mu(x)}$ and $\omega(x) \,=\, e^{i\, \tau\, \theta(x)}$, we can expand $S[U;\omega]$ (for small τ):

$$S[U;\omega] \,=\, S[U;\mathbb{1}] \,+\, \tau\, S^{'}[U;\mathbb{1}](b,x)\, \theta^b(x)$$

$$+\, \frac{\tau^2}{2}\, \theta^b(x)\, S^{''}[U;\mathbb{1}](b,x;c,y)\, \theta^c(y) \,+\, \ldots$$

where $S^{''}[U;\mathbb{1}](b,x;c,y) = \mathcal{M}(b,x;c,y)[A]$ is a lattice discretization of the Faddeev-Popov operator $-D\cdot\partial$.

Constraining the Functional Integral

At a stationary point $S^{'}[U;1\!\!1](b,x)=0$, one obtains

$$\sum_{\mu} A_{\mu}^{b}(x) \,-\, A_{\mu}^{b}(x-a\,e_{\mu}) \,=\, 0\;,$$

which is a discretized version of the (continuum) Landau gauge condition. At a local minimum

$$\mathcal{M}(b,x;c,y)[A] \geq 0\;.$$

This defines the first Gribov region $\Omega \equiv \{\,U : \partial\cdot A = 0,\, \mathcal{M} \geq 0\,\}$ (V.N. Gribov, 1978).

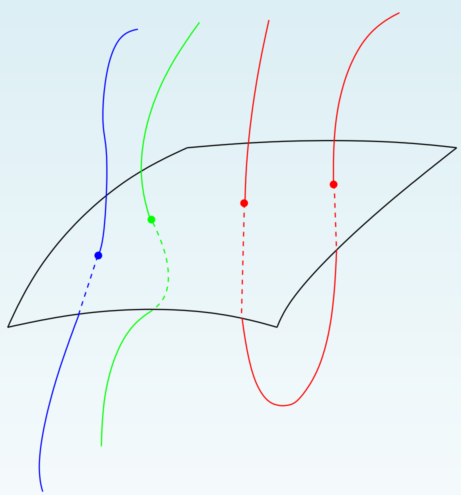

All gauge orbits intersect Ω (G. Dell'Antonio & D. Zwanziger, 1991) but the gauge fixing is not unique (Gribov copies).
Absolute minima of $S[U;\omega]$ define the fundamental modular region Λ, free of Gribov copies in its interior. (Finding the absolute minimum is a spin-glass problem.)

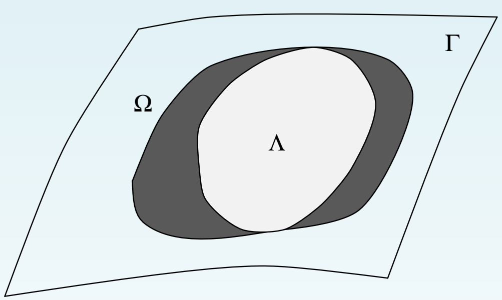

The Infinite-Volume Limit (I)

In order to study the infra-red sector of the theory on the lattice we need to remove the infra-red cutoff $\Longrightarrow$ take the infinite-volume limit.

The Main Axiom

> *At very large volumes the functional integration gets concentrated on the boundary $\partial\Omega$ of the first Gribov region Ω.*

For very large dimensionality and for large volumes, by considering the interplay among the volume of the configuration space, the Boltzmann weight and the step function used to constrain the functional integration to Ω, one expects that entropy favors configurations near the boundary $\partial\Omega$.

Gribov-Zwanziger Scenario

- The Gribov-Zwanziger confinement scenario in Landau gauge predicts a gluon propagator

$$D^{ab}_{\mu\nu}(p) \,=\, \sum_x e^{-2i\pi k\cdot x} \langle A^a_\mu(x)\, A^b_\nu(0) \rangle \,=\, \delta^{ab} \left(g_{\mu\nu} \,-\, \frac{p_\mu\, p_\nu}{p^2} \right) D(p^2)$$

  suppressed in the IR limit. In particular, $D(0) = 0$ implying that reflection positivity is maximally violated.

- This result may be viewed as an indication of gluon confinement (the propagator presents poles with complex-conjugate masses).
- Infinite volume favors configurations on the first Gribov horizon, where λ_{min} of $\mathcal{M}$ goes to zero.
- In turn, the ghost propagator

$$G(p) \,=\, \frac{1}{N_c^2 - 1} \sum_{x,\, y,\, a} \frac{e^{-2\pi i\, k\cdot(x-y)}}{V} \,\langle\, \mathcal{M}^{-1}(a, x; a, y) \,\rangle\,,$$

  should be IR enhanced, introducing long-range effects, related to the color-confinement mechanism.

Overview of Lattice Results

- Gluon propagator is suppressed in the limit $p \to 0$, while the real-space propagator violates reflection positivity.
- $\lambda_{min} \to 0$ with the volume.
- On "small" lattices: could fit to $D(0) \to 0$, observed enhancement of $G(p)$.

Studies on very large lattices presented by three groups — I.L. Bogolubsky et al. (Berlin), A. Sternbeck et al. (Adelaide), A.C. $\&$ T. Mendes (São Carlos) — at the Lattice 2007 Conference: in $3d$ and $4d$

- $D(0) > 0$, (violation of reflection positivity still holds);
- $G(p)$ shows no enhancement in the IR.
- Consistent with so-called massive solution of DSEs and refined GZ scenario.

Just before (A. Maas, 2007) in the $2d$ case:

- $D(0)$ extrapolate to zero in the infinite-volume limit;
- $G(p)$ is IR enhanced;
- consistent with scaling behavior (from DSEs) and GZ scenario.

Old Results in 3d

The $3d$ gluon propagator using lattice volumes up to 140^3 and β values $4.2, 5.0, 6.0 \longrightarrow$ physical lattice sides almost as large as 25 fm (A.C., T. Mendes & A. Taurines, 2003).

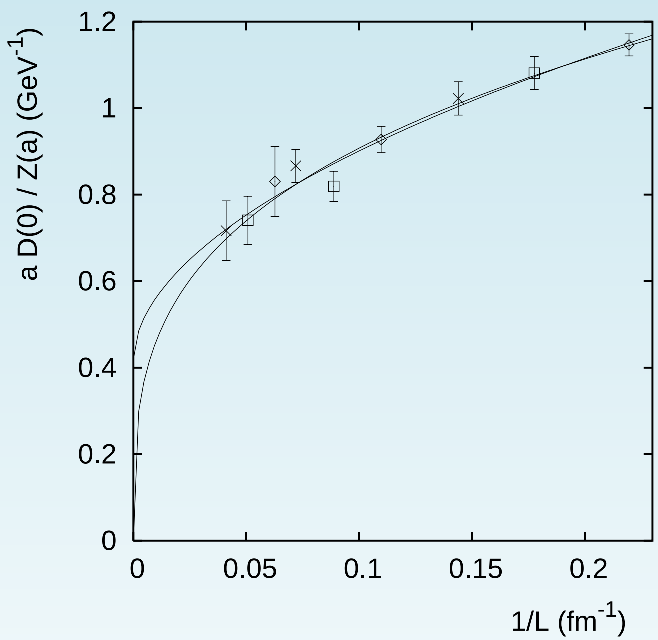

Plot of the rescaled gluon propagator at zero momentum $D(0)$ as a function of the inverse lattice side for $\beta = 4.2\,(\times)$, $5.0\,(\Box)$, $6.0\,(\Diamond)$. We also show the fit of the data using the Ansatz $d + b/L^c$ both with $d = 0$ and $d \neq 0$.

One needs to go to even larger lattice volumes!

Gluon Propagator at “Infinite” Volume

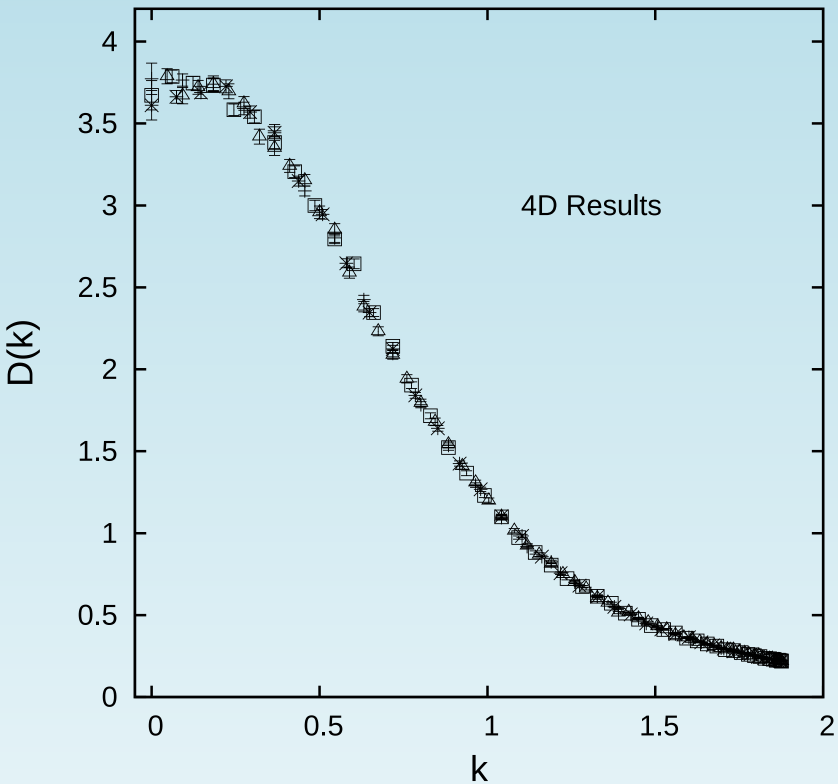

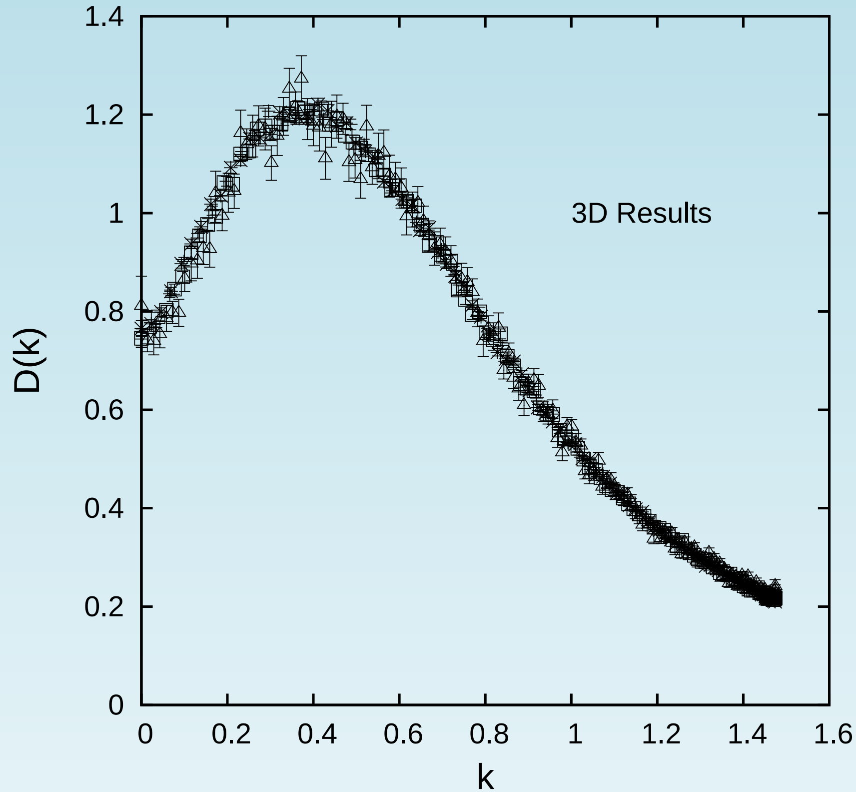

Gluon propagator $D(k)$ as a function of the lattice momenta k (both in physical units) for the pure-$SU(2)$ case in $d = 4$ (left), considering volumes of up to 128^4 (lattice extent ~ 27 fm) and $d = 3$ (right), considering volumes of up to 320^3 (lattice extent ~ 85 fm). (Data presented at LATTICE 2007.)

Violation of Reflection Positivity in 4d

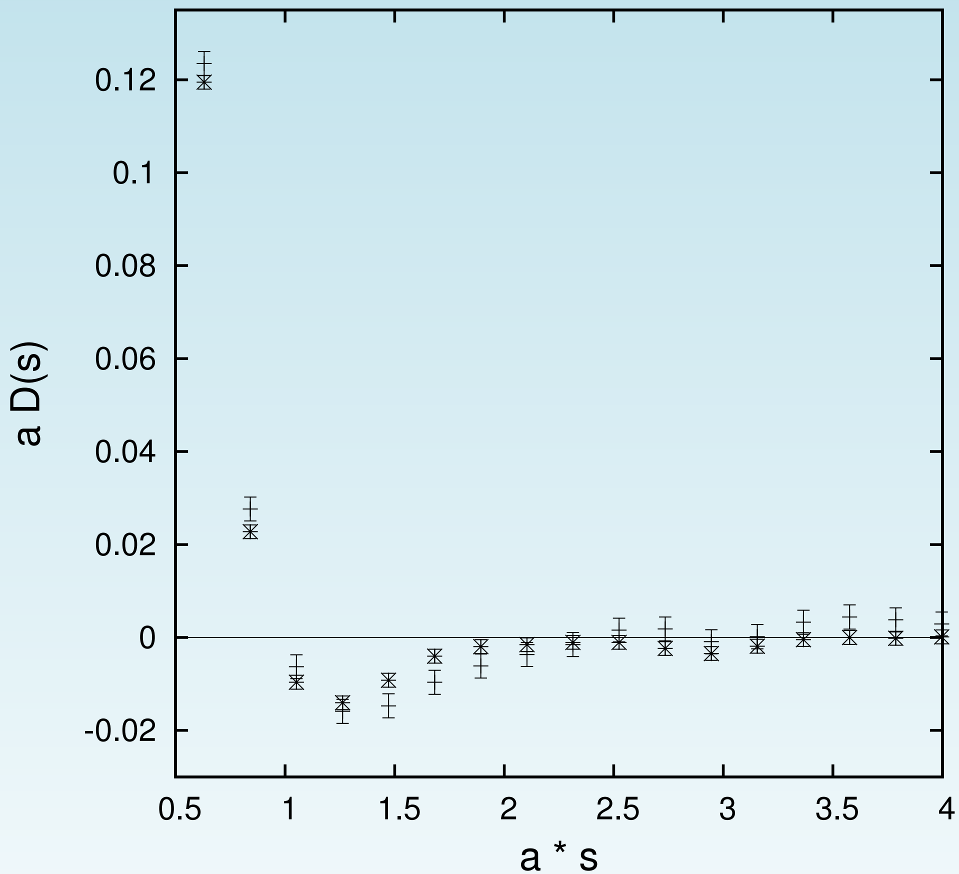

Clear violation of reflection positivity for lattice volume $V = 128^4$ at $\beta = 2.2$.

Note: this violation disappears at finite temperature for the (three-dimensional) longitudinal gluon propagator

$D_L(p) \propto \langle A_0(p)\, A_0(-p)\rangle$.

Extrapolation to Infinite Volume: a Hint

$D(0)$ vs. $1/L$

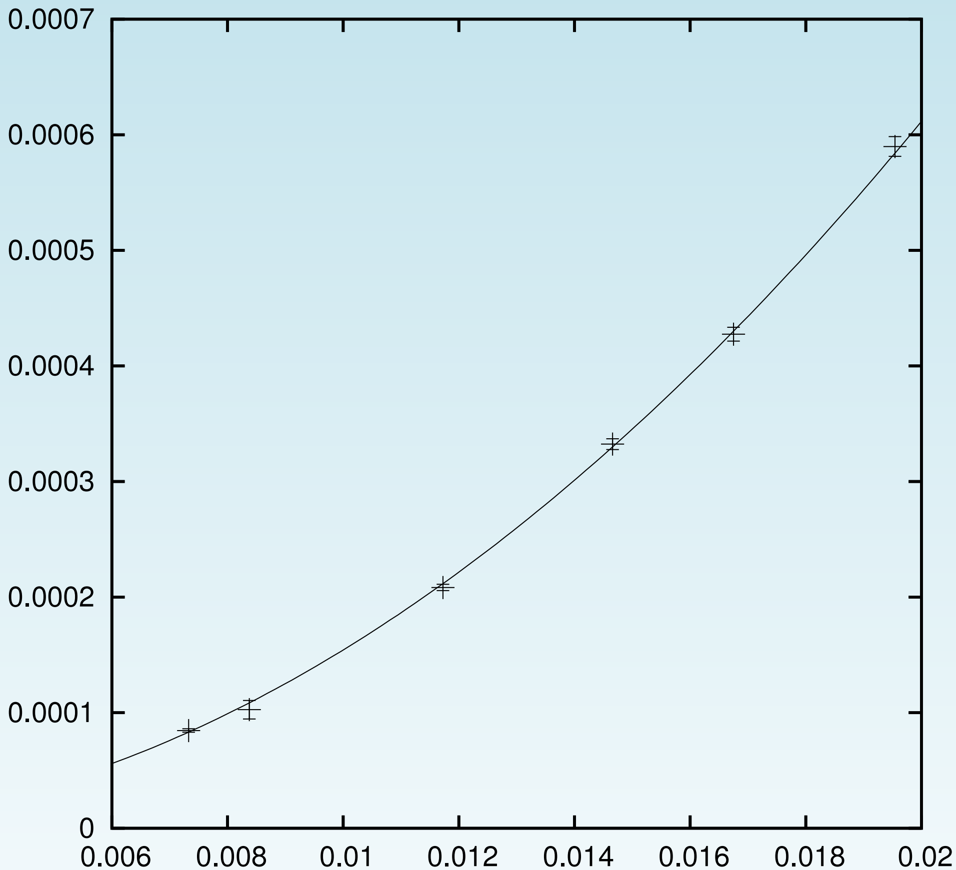

Average absolute value of the gluon field at zero momentum $|\widetilde{A}^b_\mu(0)|$ (in 4d for $\beta = 2.2$) as a function of the inverse lattice side $1/L$ (in fm^{-1}) and extrapolation to infinite volume. Recall that $D(0) \propto V \sum_{\mu,b} |\widetilde{A}^b_\mu(0)|^2$. We also show the fit of the data using the Ansatz b/L^c (with $c = 1.99 \pm 0.02$).

Zwanziger proved (1991) that in Landau gauge this quantity should go to zero at least as fast as $1/L$.

Bounds for $D(0)$

We can obtain upper and lower bounds for the gluon propagator at zero momentum $D(0)$ by considering the quantity

$$\overline{M}(0) \;=\; \frac{1}{d(N_c^2-1)} \sum_{b,\mu} |\widetilde{A}^b_\mu(0)| \;.$$

Indeed, one can prove that (A.C. & T. Mendes, 2008)

$$V \,\langle \overline{M}(0) \rangle^2 \;\leq\; D(0) \;\leq\; V d(N_c^2-1)\,\langle \overline{M}(0)^2 \rangle \;.$$

Thus, if $\overline{M}(0)$ goes to zero as $V^{-\alpha}$ we find that

$$D(0) \to 0, \quad 0 < D(0) < +\infty \quad \text{or} \quad D(0) \to +\infty$$

respectively if α is larger than, equal to or smaller than 1/2.

Upper and Lower Bounds for $D(0)$ (I)

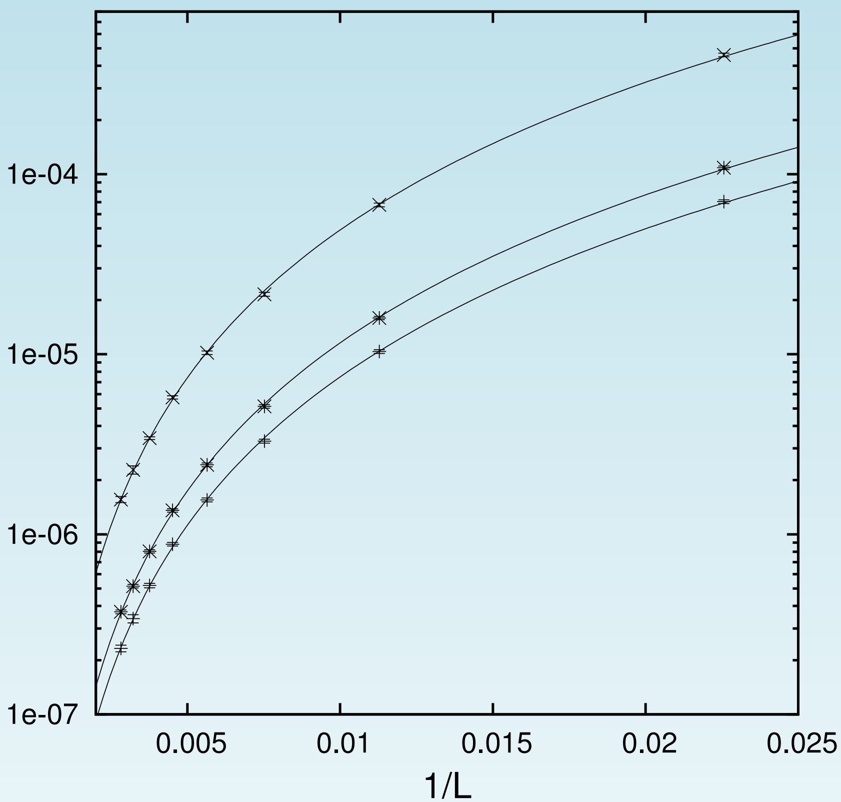

Two-dimensional case: B_l/L^l (for $a\langle\overline{M}(0)\rangle$) and the Ansatz B_u/L^u (for $a^2\langle\,\overline{M}(0)^2\,\rangle$), with $B_l = 1.48(6)$, $l = 1.367(8)$ and $\chi/d.o.f. = 1.00$ and $B_u = 2.3(2)$, $u = 2.72(1)$ and $\chi/d.o.f. = 1.02$.

Upper and lower bounds extrapolate to zero faster than $1/V$, implying $D(0) = 0$.

Upper and Lower Bounds for $D(0)$ (II)

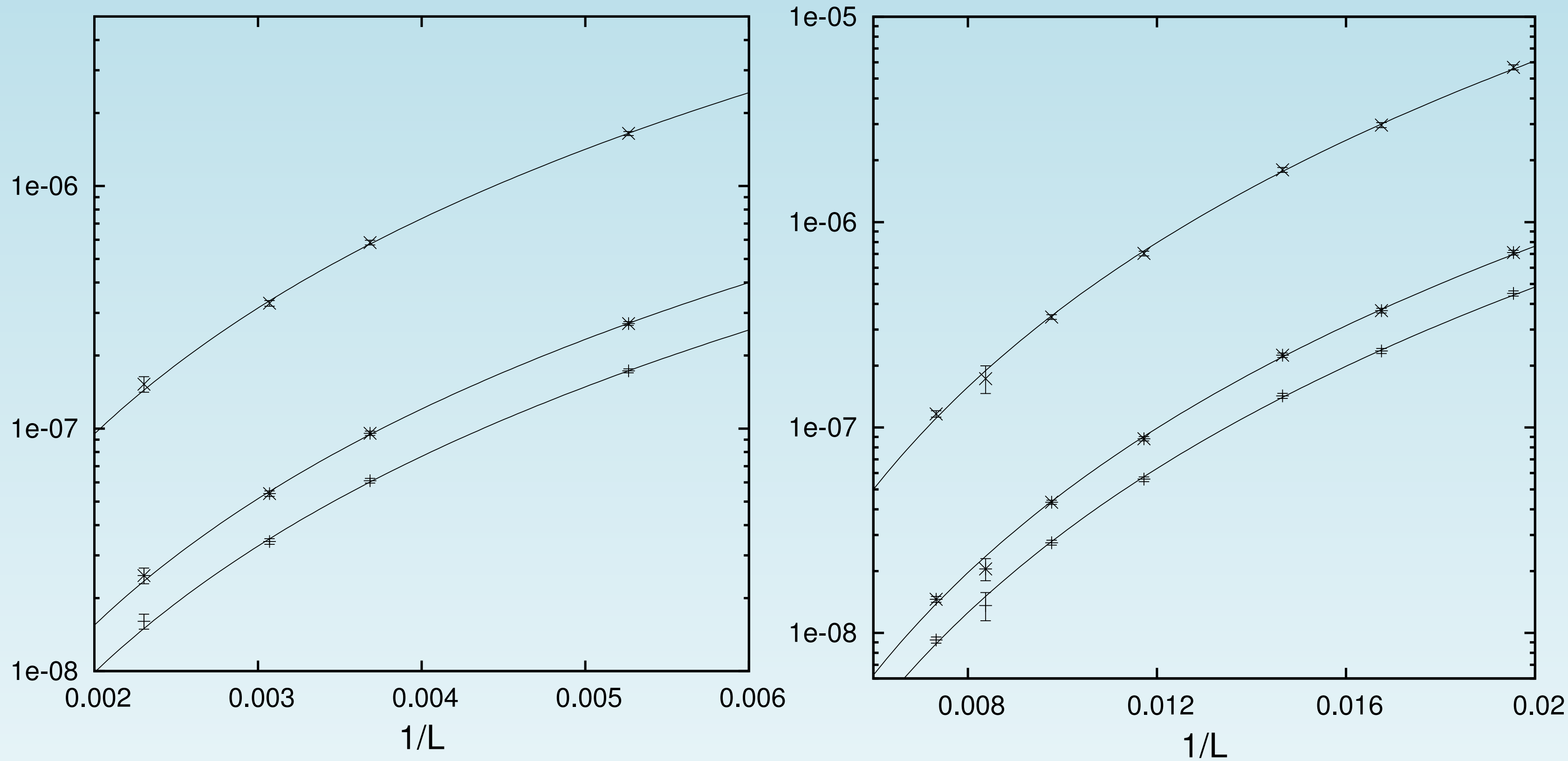

Similarly for 3d: $l = 1.48(3)$ and $u = 2.95(5)$ ($\chi/d.o.f. = 0.95$).

Similarly for 4d: $l = 1.99(2)$ and $u = 3.99(4)$ ($\chi/d.o.f. = 0.96$).

Upper / lower bounds extrapolate to zero as $1/V$, implying $D(0) > 0$.

Gluon Propagator at Infinite Volume

- Violation of reflection positivity in 2d, 3d and in 4d.
- Gluon propagator in Landau gauge IR finite in 3d and 4d, as a consequence of "self-averaging" of a magnetization-like quantity [i.e. $M(0)$].
- May think of $D(0)$ as a response function (susceptibility) of this observable ("magnetization"). In this case it is natural to expect $D(0) \sim const$ in the infinite-volume limit.
- Finite $D(0)$ value explained considering randomly oriented domains (F. Gutbrod, 1996).
- 2d case is different, the magnetization is "over self-averaging", the susceptibility is zero.

Question: why is the 2d case different?

No-Pole Condition (I)

The restriction of the functional integration to the first Gribov region $\Omega \equiv \{\, U : \partial \cdot A = 0,\, \mathcal{M} \geq 0 \,\}$ should imply for the ghost propagator

$$G(p) = \frac{1}{N_c^2 - 1} \sum_{x,\, y,\, a} \frac{e^{-2\pi i\, k \cdot (x-y)}}{V} \langle\, \mathcal{M}^{-1}(a, x; a, y) \,\rangle = \frac{1}{p^2} \frac{1}{1 - \sigma(p^2)}$$

that (no-pole condition)

$$\sigma(p^2) < 1 \qquad \text{for} \qquad p^2 > 0 \; .$$

By considering the one-loop-corrected ghost propagator

$$G(p^2) = \frac{1}{p^2} - \frac{\delta^{ab}}{N^2 - 1} \frac{1}{p^4} g_0^2 f^{adc} f^{cdb} \int \frac{d^d q}{(2\pi)^d} \, (p-q)_\mu \, p_\nu \, D(q^2) \, P_{\mu\nu}(q) \, \frac{1}{(p-q)^2}$$

one has

$$\sigma(p^2) = g_0^2 N \frac{p_\mu p_\nu}{p^2} \int \frac{d^d q}{(2\pi)^d} \frac{1}{(p-q)^2} D(p^2) \, P_{\mu\nu}(q) \; .$$

No-Pole Condition (II)

Under general hypothesis, one can show that (A. C., D. Dudal, & N. Vandersickel, 2012)

$$\frac{\sigma(0)}{g_0^2 N} = \frac{1}{8\pi}\left\{\mathcal{D}(0) - \lim_{k^2\to 0} \ln\left(k^2\right)\mathcal{D}(0) + \int_0^\infty dx\,\left[x\ln\left(x\right) - x\right]\mathcal{D}''(x)\right\}$$

and there is a small-momentum singularity proportional to $-\mathcal{D}(0)\ln\left(k^2\right)$. Thus, the no-pole condition requires $D(0) = 0$ in $2d$!

In the general d-dimensional case one finds

$$\frac{\sigma(p^2)}{g_0^2 N} = \frac{\Omega_d}{(2\pi)^d}\,\frac{d-1}{d}\int_0^\infty dq\, q^{d-1}\, D(q^2)\left[\frac{\theta(p^2-q^2)}{p^2}\,{}_2F_1\left(1, 1-d/2; 1+d/2; q^2/p^2\right)\right.$$

$$\left. + \frac{\theta(q^2-p^2)}{q^2}\,{}_2F_1\left(1, 1-d/2; 1+d/2; p^2/q^2\right)\right]\,,$$

where ${}_2F_1(a, b; c; z)$ is the Gauss hypergeometric function. One can verify that only in the $2d$ case is the above result ill-defined if $D(0) > 0$.

The above results can be proven also considering the DSE for $\sigma(p^2)$.

What about

the Ghost Propagator?

(A.C. & T. Mendes, 2008 and 2013)

Ghost Fits (I)

Fit of the ghost dressing function $p^2G(p^2)$ as a function of p^2 (in GeV) for the 2d case ($\beta = 10$ with volume 320^2). We find that $p^2G(p^2)$ is best fitted by the form $p^2G(p^2) = a(p^{-2k} + bp^{2e})/(1 + p^{2e})$,

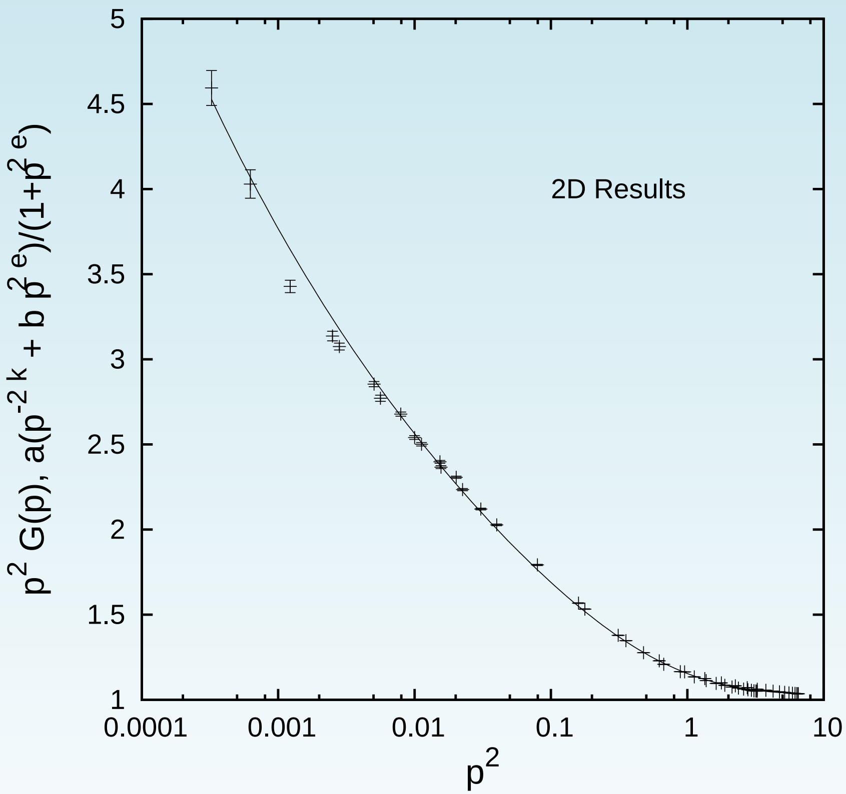

with:

$a = 1.24(3)\, GeV^{2(e+\kappa)}$

$\kappa = 0.16(2)$

$b = 0.86(3)\, GeV^{-2(e+\kappa)}$

$e = 0.75(15)$.

In the infrared limit $p^2G(p^2) \sim p^{-2k}$.

Ghost Fits (II)

Fit of the ghost dressing function $p^2G(p^2)$ as a function of p^2 (in GeV) for the 3d case ($\beta = 3$ with volume 240^3). We find that $p^2G(p^2)$ is best fitted by the form $p^2G(p^2) = a - b[\log(1 + cp^2) + dp^2]/(1 + p^2)$,

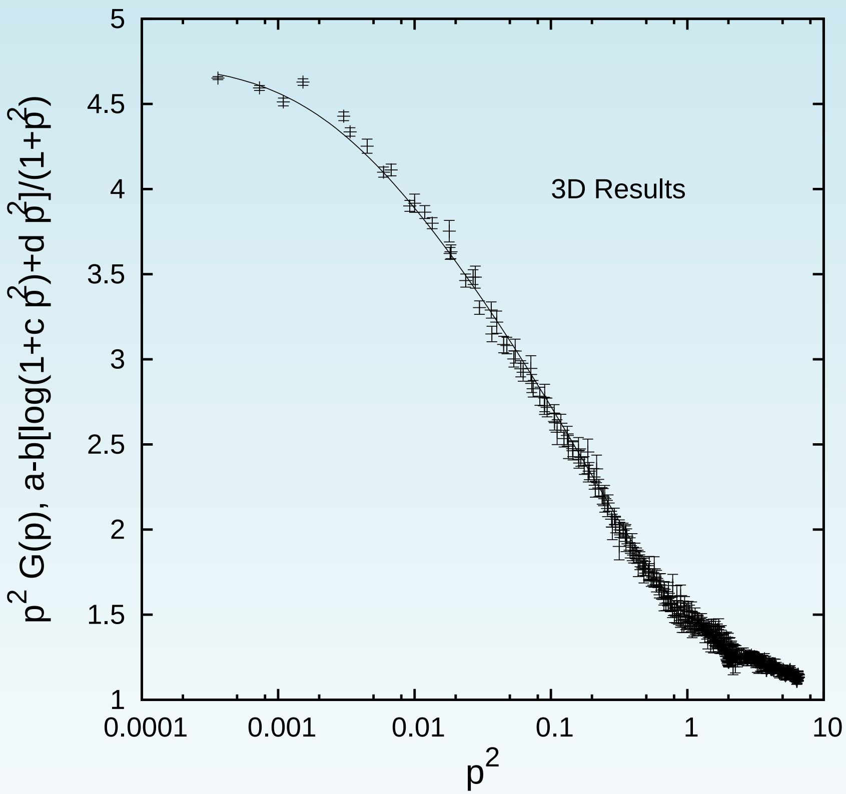

with:

$a = 4.75(1)$

$b = 0.491(5)\, GeV^2$

$c = 450(30)\, GeV^{-2}$

$d = 7.1(1)\, GeV^{-2}$.

In the infrared limit $p^2G(p^2) \sim a$.

Ghost Fits (III)

Fit of the ghost dressing function $p^2 G(p^2)$ as a function of p^2 (in GeV) for the 4d case ($\beta = 2.2$ with volume 80^4). We find that $p^2 G(p^2)$ is best fitted by the form $p^2 G(p^2) = a - b[\log(1 + cp^2) + dp^2]/(1 + p^2)$,

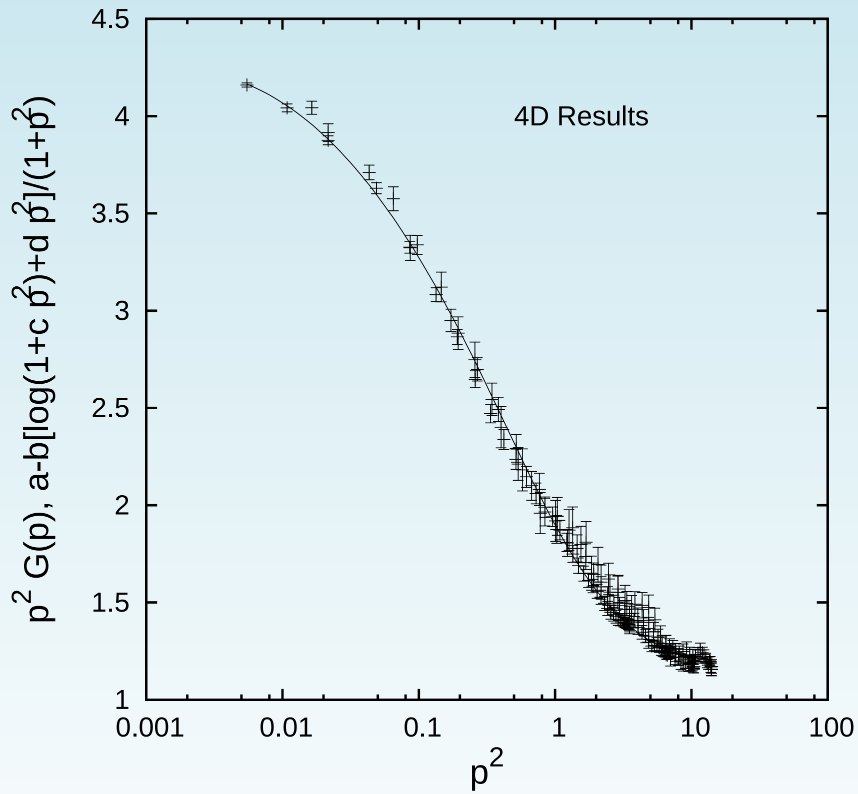

with:

$a = 4.32(2)$

$b = 0.38(1)\, GeV^2$

$c = 80(10)\, GeV^{-2}$

$d = 8.2(3)\, GeV^{-2}$.

In the infrared limit $p^2 G(p^2) \sim a$.

Ghost Propagator at Infinite Volume

From present fits we have for the ghost dressing function $p^2 G(p^2)$ an IR behavior $\sim p^{-2k}$ with

- $k \approx 0.16$ in $2d$,
- $k \approx 0$ in $3d$ and in $4d$.

Can we explain the difference between the $2d$ and the 3 and $4d$ cases?

Upper and Lower Bounds for $G(p)$ (I)

Consider eigenvectors $\psi_i(a,x)$ and associated eigenvalues λ_i of the FP matrix $\mathcal{M}(a,x;b,y)$. In Landau gauge the eigenvectors corresponding to null λ are constant modes.

One can prove that, for any nonzero momentum p

$$\frac{1}{N_c^2-1}\,\frac{1}{\lambda_1}\sum_a |\widetilde{\psi}_1(a,p)|^2 \,\leq\, G(p) \,\leq\, \frac{1}{\lambda_1}\;,$$

where λ_1 is the smallest nonzero eigenvalue.

Now, assuming the power-law behavior $p^{-2-2\kappa}$ for the ghost propagator in the IR limit, using $p_{min} \propto 1/L$ and under the hypothesis that $\lambda_1 \sim L^{-\alpha}$ in the infinite-volume limit, we expect to have

$$2 + 2\kappa \,\leq\, \alpha$$

and a necessary condition for IR enhancement of $G(p)$ is

$$\alpha \,>\, 2\,.$$

Upper Bounds for $G(p)$

The ghost propagator $G(p_{min})$ for the smallest nonzero momentum $p_{min} = 2\sin(\pi/N)$ and $1/\lambda_1$ (both in GeV^{-2}) as a function of the inverse lattice side $1/L$ (GeV).

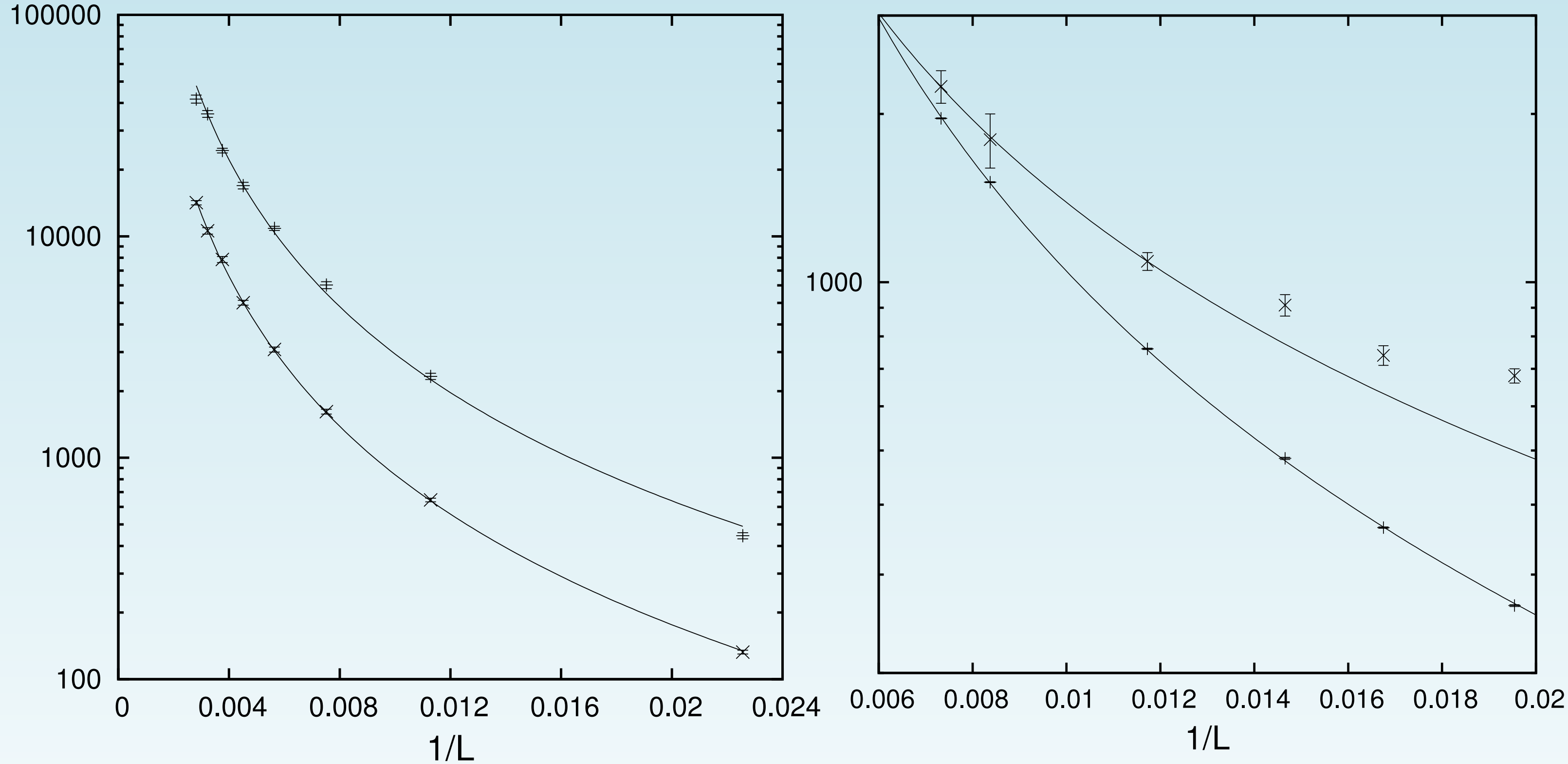

For 2d: $2\kappa = 0.251(9)$, $\alpha = 2.20(4)$. For 4d: $2\kappa = 0.043(8)$, $\alpha = 1.53(2)$.

Upper and Lower Bounds for $G(p)$ (II)

The above results can be sistematically improved, for example by considering the second smallest nonzero eigenvalue λ_2 of the FP matrix:

$$\frac{1}{N_c^2 - 1} \sum_b \left[\frac{1}{\lambda_1} \, |\widetilde{\psi}_1(b,p)|^2 + \frac{1}{\lambda_2} \, |\widetilde{\psi}_2(b,p)|^2 \right] \leq G(p)$$

and

$$G(p) \leq \left(\frac{1}{\lambda_1} - \frac{1}{\lambda_2} \right) \left(\frac{1}{N_c^2 - 1} \sum_b |\widetilde{\psi}_1(b,p)|^2 \right) + \frac{1}{\lambda_2} \; .$$

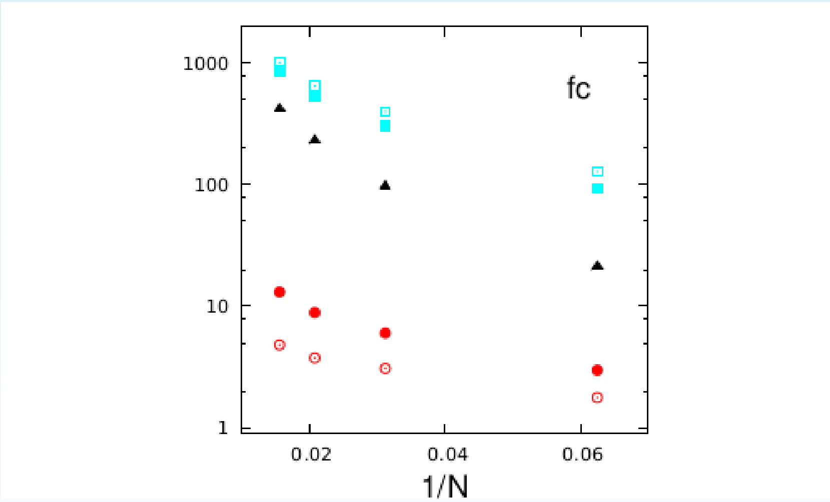

The ghost propagator $G(p_{min})$ (full triangles), the two lower bounds (respectively empty and full circles) and the two upper bounds (respectively empty and full squares) as a function of the inverse lattice size $1/N$ with $N = 16, 32, 48$ and 64 for the SU(2) case at $\beta = 2.2$. All quantities are in lattice units.

The Infinite-Volume Limit (II)

New Axiom Formulation

> *The key point seems to be the rate at which λ_1 goes to zero, which, in turn, should be related to the rate at which a thermalized and gauge-fixed configuration approaches $\partial\Omega$.*

These are only qualitative statements!

How do we relate λ_1
to the geometry of the Gribov region Ω ?

The Region Ω: Properties

Three important properties have been proven (D. Zwanziger, 1982) for the Gribov region Ω:

1. the trivial vacuum $A_\mu = 0$ belongs to Ω;
2. the region Ω is convex;
3. the region Ω is bounded in every direction.

(The same properties can be proven also for the fundamental modular region Λ.)

The first property is trivial, since $A_\mu = 0$ implies that $\mathcal{M}(b, x; c, y)[0]$ is (minus) the Laplacian $-\partial^2$ (which is a semi-positive-definite operator).

Lower bound for λ_1

Consider a configuration A' belonging to the boundary $\partial\Omega$ of Ω. From the second property, $A = \rho A' \in \Omega$ for $\rho \in [0,1]$. Then, by using the concavity of the minimum function one can show that

$$\lambda_1 \left[\mathcal{M}[A] \right] \geq [1 - \rho(A)] \, p^2_{min} \; .$$

Here $1-\rho(A) \leq 1$ measures the distance of a configuration $A \in \Omega$ from the boundary $\partial\Omega$ (in such a way that $\rho^{-1} A \in \partial\Omega$). This result applies to any Gribov copy belonging to Ω.

As the lattice side L goes to infinity, $\lambda_1 \left[\mathcal{M}[A] \right]$ cannot go to zero faster than $[1 - \rho(A)] \, p^2_{min}$. Since $p^2_{min} \sim 1/L^2$ at large $L \Longrightarrow \lambda_1$ behaves as $L^{-2-\alpha}$ in the same limit, with $\alpha > 0$, only if $1 - \rho(A)$ goes to zero at least as fast as $L^{-\alpha}$.

In the Abelian case one has $\mathcal{M} = -\partial^2$ and $\lambda_1 = p^2_{min}$.
$\Longrightarrow$ All non-Abelian effects are included in the $[1 - \rho(A)]$ factor
(and in the inequality).

Simulating the Math

We used 70 configurations, for the SU(2) case at $\beta = 2.2$, for $V = 16^4$, $24^4, 32^4, 40^4$ and 50 configurations for $V = 48^4, 56^4, 64^4, 72^4, 80^4$.

In order to verify the third property of the region Ω we applied scale transformations $\widehat{A}_\mu^{(i)}(x) = \tau_i A_\mu^{(i-1)}(x)$ to the gauge configuration A with

- $\tau_0 = 1$,
- $\tau_i = \delta\, \tau_{i-1}$,
- $\delta = 1.001$ if $\lambda_1 \geq 5 \times 10^{-3}$,
- $\delta = 1.0005$ if $\lambda_1 \in [5 \times 10^{-4}, 5 \times 10^{-3})$
- and $\delta = 1.0001$ if $\lambda_1 < 5 \times 10^{-4}$,

where λ_1 is evaluated at the step $i - 1$.

After n steps, the modified gauge field $\widehat{A}_\mu^{(n)}(x)$ does not belong anymore to the region Ω, i.e. the eigenvalue λ_1 of $\mathcal{M}[\widehat{A}^{(n)}]$ is negative (while λ_2 is still positive).

Check the New Inequality

Using $A' = \widetilde{\tau}\, A \equiv A(\tau_{n-1} + \tau_n)/2 \in \partial\Omega$ and $\rho = 1/\widetilde{\tau} < 1$:

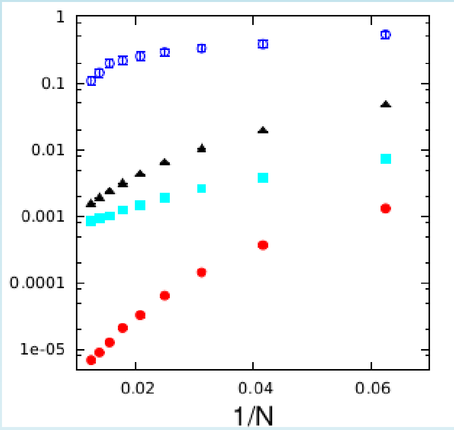

plot of the inverse of the lower bound (**empty circles**), of $1/G(p_{min})$ (**full triangles**), of λ_1 (**full squares**) and of the quantity $(1 - \rho)\, p_{min}^2$ (**full circles**) as a function of the inverse lattice size $1/N$.

The new inequality $\lambda_1\, [\, \mathcal{M}[A]\,] \geq [1 - \rho(A)]\, p_{min}^2$ becomes an equality if and only if the eigenvectors corresponding to the smallest nonzero eigenvalues of $\mathcal{M}[A]$ and $-\partial^2$ coincide.

$\Longrightarrow$ The eigenvector ψ_{min} is very different from the plane waves corresponding to p_{min}.

These results explain the non-enhancement of $G(p)$ in the IR.

Summary

Our new bounds suggest all non-perturbative features of a minimal-Landau-gauge configuration $A \in \Omega$ to be related to its normalized distance ρ from the "origin" $A = 0$ or, equivalently, to its normalized distance $1 - \rho$ from the boundary $\partial\Omega$.

We now begin to understand why no ghost enhancement (scaling solution) is seen on the lattice (in the $3d$ and $4d$ case.

We still do not have a full understanding of why the $2d$ case is different.

Conclusion

We have not succeeded in answering all our problems. The answers we have found only serve to raise a whole set of new questions. In some ways we feel we are as confused as ever, but we believe we are confused on a higher level and about more important things.

In: *Stochastic Differential Equations: An Introduction with Applications*,
Bernt Øksendal

Some Extra Stuff

Quantum Chromodynamics (QCD)

QCD Lagrangian is just like the one of QED:

quarks (spin-1/2 fermions)	$\Leftrightarrow$	electrons
gluons (vector bosons) / color charge		photons / electric charge

But: gauge symmetry is $SU(3)$ (non-Abelian) instead of $U(1)$

$$\mathcal{L} \;=\; -\frac{1}{4}\, F^{a}_{\mu\nu}\, F_{a}^{\mu\nu} \,+\, \sum_{f=1}^{6} \bar{\psi}_{f,i} \left(i\,\gamma^{\mu}\, D_{\mu}^{ij} - m_f\,\delta_{ij}\right) \psi_{f,j}$$

where [$a = 1,\ldots,8$; $i = 1,\ldots,3$; T^a_{ij} are the $SU(3)$ generators]

$$F^{a}_{\mu\nu} \;\equiv\; \partial_{\mu} A^{a}_{\nu} - \partial_{\nu} A^{a}_{\mu} + g_0\, f_{abc}\, A^{b}_{\mu}\, A^{c}_{\nu}$$

$$D_{\mu} \;\equiv\; \partial_{\mu} - i\, g_0\, A^{a}_{\mu}\, T_a$$

Invariant under local gauge transformations

$$A^{\Omega}_{\mu}(x) \;=\; \Omega(x) A_{\mu}(x) \Omega^{-1}(x) - \frac{i}{g_0} \left[\partial_{\mu}\Omega(x)\right] \Omega^{-1}(x)$$

$$\psi^{\Omega}_{f}(x) \;=\; \Omega(x)\psi_f(x)$$

where $\Omega(x) = \exp\left[-i g_0 \Lambda^a(x) T_a\right] \;\in\; SU(3)$.

Origin of Confinement

Note: $F^a_{\mu\nu} \sim g_0 \, f^{abc} \, A^b_\mu \, A^c_\nu$

$\Rightarrow$ QCD Lagrangian contains terms with three and four gauge fields in addition to quadratic terms (propagators).

$\mathcal{L}_{\bar{\psi}\psi A} = g_0 \, \bar{\psi} \, \gamma^\mu A_\mu \, \psi \Rightarrow$ quark-quark-gluon vertex

$\mathcal{L}_{AAA} = g_0 \, f^{abc} \, A^\mu_a \, A^\nu_b \, \partial_\mu A^c_\nu \Rightarrow$ three-gluon vertex

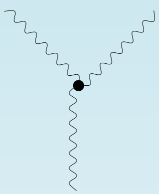

$\Rightarrow$ Gluons interact with each other (have color charge), determining the peculiar properties and the nonperturbative nature of low-energy QCD.

$\Rightarrow$ Running coupling $\alpha_s(p)$: the strength of the interaction increases for larger r (smaller p) and vice-versa (confinement vs. aymptotic freedom). Perturbation theory breaks down in the limit of small energies.

3-Step Code

```
main()
{
/* set parameters: beta, number of configurations NC,
                  number of thermalization sweeps NT */
     read_parameters();
/* {U} is the link configuration */
     set_initial_configuration(U);
/* cycle over NC configurations */
     for (int c=0; c < NC; c++) {
          thermalize(U,NT);
          gauge_fix(U,g);
          evaluate_propagators_and_vertices(U);
     }
}
```

Parallelization

- We need a parallelized code in order to simulate at very large lattice volumes V.
- Communication is required in each of the three steps.
- Each node gets a contiguous block of $v = V/N$ lattice sites (local lattice).
- Communication is required only for sites on the boundary of the local lattice.
- 4D simulations $\rightarrow$ high granularity due to the surface/volume effect.

Weak and Strong Scaling on BG/Q

V	Nodes	HB	Micro	Gfix	GluonProp	CG
$64^2 \times 32^2$	32	494.9	54.7	0.0044	0.041	0.0081
$64^3 \times 32$	64	496.3	62.1	0.0049	0.041	0.0088
64^4	128	496.8	59.2	0.0047	0.050	0.0084
$64^3 \times 128$	256	499.4	63.0	0.0050	0.041	0.0090
$64^2 \times 128^2$	512	499.7	56.4	0.0046	0.042	0.0083
64^4	128	496.8	59.2	0.0047	0.0050	0.0084
64^4	256	256.3	37.9	0.0029	0.0028	0.0055
64^4	512	134.6	27.3	0.0020	0.0018	0.0040
64^4	1024	74.4	22.5	0.0016	0.0012	0.0035
64^4	512	2943.6	218.5	0.0171	0.0179	0.0239

Weak (with 5 different lattice volumes) and strong (with 4 different volumes) scaling: time (in seconds) for 3 different updates of local variables and for the evaluation of the gluon propagator and the time (in seconds) for one conjugate gradient iteration. Link and site variables are SU(2) matrices. The last row is for the BG/P.

Breaking of Rotational Invariance

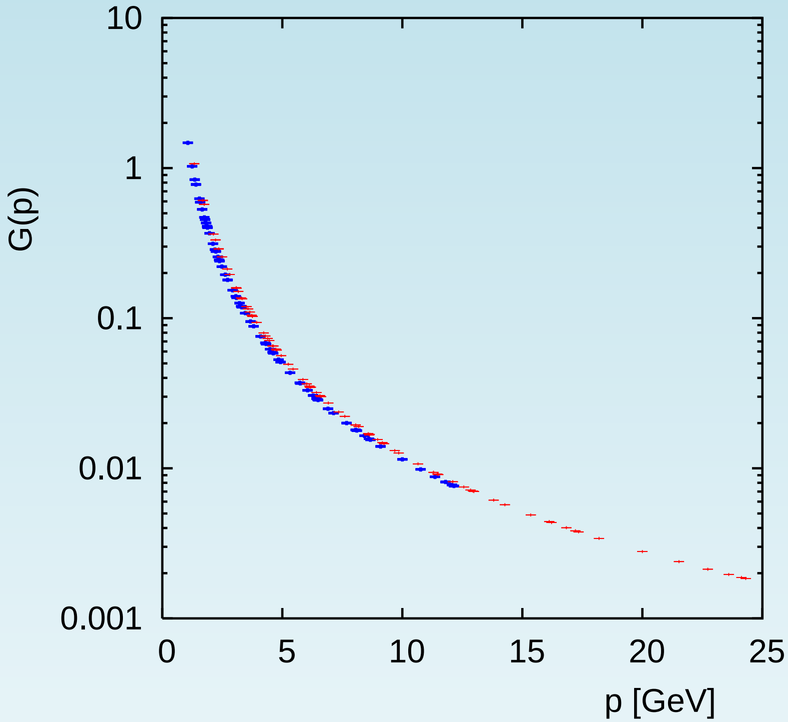

Ghost propagator (in Landau gauge) for two different sets of momenta [$V = 26^4$, SU(2) case].

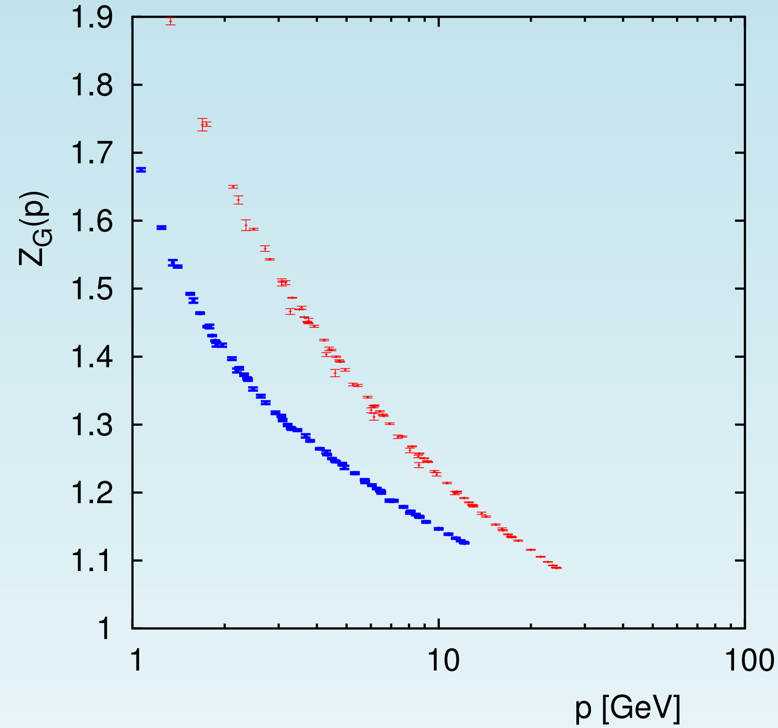

Ghost propagator (in Landau gauge) multiplied by p^2 for two different sets of momenta [$V = 26^4$, SU(2) case].

Bounds for $D(0)$ (I)

Consider the Cauchy-Bunyakovski-Schwarz inequality $|\vec{X}\cdot\vec{Y}|^2 \leq \|\vec{X}\|^2\|\vec{Y}\|^2$, a vector $\vec{Y}$ with all components equal to 1 and a vector $\vec{X}$ with components X_i. We find

$$\left(\frac{1}{m}\sum_{i=1}^{m} X_i\right)^2 \;\leq\; \frac{1}{m}\sum_{i=1}^{m} X_i^2 \;,$$

where m is the number of components of the vectors $\vec{X}$ and $\vec{Y}$. We can apply this inequality first to the vector with $m = d(N_c^2-1)$ components $\langle|\widetilde{A}_\mu^b(0)|\rangle$, where $\widetilde{A}_\mu^b(0) = V^{-1}\sum_x A_\mu^b(x)$ is the gluon field at zero momentum. This yields

$$\langle\overline{M}(0)\rangle^2 \;\leq\; \frac{1}{d(N_c^2-1)}\sum_{b,\mu}\langle|\widetilde{A}_\mu^b(0)|\rangle^2 \;.$$

Then, we can apply the same inequality to the Monte Carlo estimate of the average value

$$\langle|\widetilde{A}_\mu^b(0)|\rangle \;=\; \frac{1}{n}\sum_c |\widetilde{A}_{\mu,c}^b(0)| \;,$$

where n is the number of configurations. In this case we obtain

$$\langle|\widetilde{A}_\mu^b(0)|\rangle^2 \;\leq\; \langle|\widetilde{A}_\mu^b(0)|^2\rangle \;.$$

Bounds for $D(0)$ (II)

Thus, by recalling that

$$D(0) \;=\; \frac{V}{d(N_c^2-1)} \sum_{b,\mu} \langle |\widetilde{A}^b_\mu(0)|^2 \rangle \;,$$

and that

$$\overline{M}(0) \;=\; \frac{1}{d(N_c^2-1)} \sum_{b,\mu} |\widetilde{A}^b_\mu(0)|$$

we find

$$\left[V^{1/2} \langle \overline{M}(0) \rangle \right]^2 \;\leq\; D(0) \;.$$

We can now consider the inequality

$$\langle \sum_{\mu,b} |\widetilde{A}^b_\mu(0)|^2 \rangle \;\leq\; \langle \Big\{ \sum_{\mu,b} |\widetilde{A}^b_\mu(0)| \Big\}^2 \rangle \;.$$

This implies

$$D(0) \;\leq\; V d(N_c^2-1) \, \langle \overline{M}(0)^2 \rangle \;.$$

Bound for $D(0)$ (III)

The fit $\mathcal{A}(0) \sim 1/\sqrt{V}$ and a finite value for the gluon propagator at zero momentum $D(0)$ can be explained (F. Gutbrod, 1996) by considering randomly orientated domains of volume V_d with an average value

$$\overline{A_d(0)} \;=\; \frac{1}{V_d} \sum_{x \in V_d} A_\mu^b(x) \;,$$

essentially independent of b, μ and of the considered domain. Then, we have a number of domains $N_d = V/V_d$ and in the limit of N_d going to infinity we should find that

$$A(0) \;=\; \frac{1}{N_d} \sum_d \overline{A_d(0)}$$

is zero with a standard deviation of the order of $1/\sqrt{N_d} \sim 1/\sqrt{V}$. This is indeed the case, both in 3d and in 4d.

Bound for $D(0)$ (IV)

At the same time, one should recall that given a Gaussian random variable x with null mean value and standard deviation σ, the random variable $|x|$ has mean value (and standard deviation) proportional to σ. In our case, this means that the average value of the quantity $\mathcal{A}(0)$ should be proportional to $1/\sqrt{V}$, as indeed shown by our data. At the same time, we have that

$$D(0) = V \langle \sigma^2_{A(0)} \rangle = \frac{V}{N_d^2} \sum_d \langle \sigma^2_{A_d(0)} \rangle = \frac{V}{N_d} \langle \sigma^2_{A_d(0)} \rangle = V_d \langle \sigma^2_{A_d(0)} \rangle \; .$$

After averaging over Monte Carlo configurations we have

$$\langle \sigma^2_{A_d(0)} \rangle \; = \; \langle [A_d(0)]^2 \rangle \; .$$

Gutbrod founded $V_d \approx 14^4$. This is relatively large and it could explain why the fluctuations for $D(0)$ are usually quite large and why one needs very large lattice volumes.

Bounds for $G(p)$ (I)

Consider eigenvectors $\psi_i(a,x)$ and associated eigenvalues λ_i of the FP matrix $\mathcal{M}(a,x;b,y)$. The ψ's form a complete orthonormal set

$$\sum_{i=1}^{(N_c^2-1)V} \psi_i(a,x)\,\psi_i(b,y)^* \;=\; \delta_{ab}\delta_{xy} \quad \text{and} \quad \sum_{a,x} \psi_i(a,x)\,\psi_j(a,x)^* \;=\; \delta_{ij}\;.$$

If we now write

$$\mathcal{M}^{-1}(a,x;b,y) \;=\; \sum_{i,\lambda_i\neq 0} \frac{1}{\lambda_i}\psi_i(a,x)\,\psi_i(b,y)^*\;,$$

we get for $G(p)$ the expression

$$G(p) \;=\; \frac{1}{N_c^2-1}\sum_{i,\lambda_i\neq 0}\frac{1}{\lambda_i}\sum_a |\widetilde{\psi}_i(a,p)|^2\;,$$

where

$$\widetilde{\psi}_i(a,p) \;=\; \frac{1}{\sqrt{V}}\sum_x \psi_i(a,x)\,e^{-2\pi i k\cdot x}\;.$$

Bounds for $G(p)$ (II)

From the above expression we immediately get for $G(p)$ the bounds

$$\frac{1}{N_c^2 - 1} \, \frac{1}{\lambda_{min}} \, \sum_a |\widetilde{\psi}_{min}(a,p)|^2 \leq G(p)$$

and

$$G(p) \leq \frac{1}{N_c^2 - 1} \, \frac{1}{\lambda_{min}} \, \sum_{i, \lambda_i \neq 0} \, \sum_a \, |\widetilde{\psi}_i(a,p)\,|^2 \; .$$

Now by adding and subtracting the contribution from the null eigenvalue and using the completeness relation, the upper bound may be rewritten as

$$G(p) \; \leq \; \frac{1}{\lambda_{min}} \, \left[1 \, - \, \frac{1}{N_c^2 - 1} \sum_{j, \lambda_j = 0} \, \sum_a \, |\widetilde{\psi}_j(a,p)\,|^2 \right] \; .$$

In Landau gauge the eigenvectors corresponding to null λ are constant modes. Thus for any nonzero p we have

$$\frac{1}{N_c^2 - 1} \, \frac{1}{\lambda_{min}} \, \sum_a \, |\widetilde{\psi}_{min}(a,p)|^2 \; \leq \; G(p) \; \leq \; \frac{1}{\lambda_{min}} \; .$$

The Infinite-Volume Limit (III)

One can check if lattice data support $\lambda_1[A] \to 0$ in the infinite-volume limit $\Longrightarrow A \in \partial\Omega$.

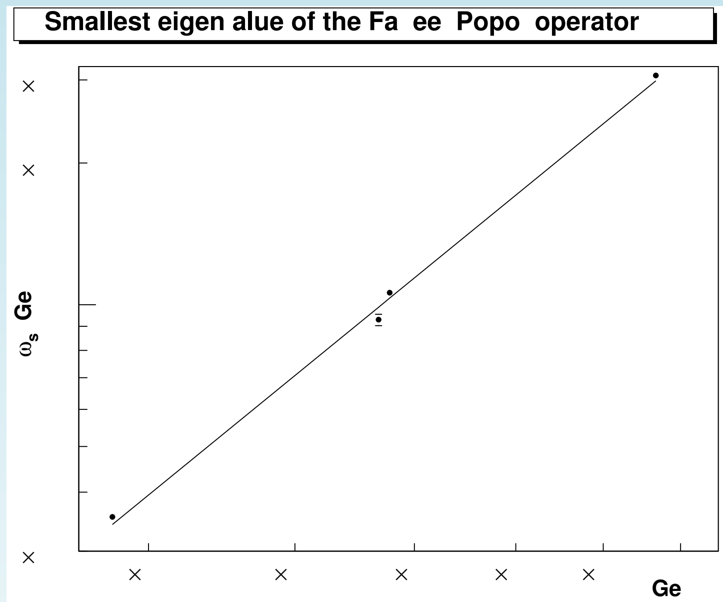

Infinite-volume limit extrapolation $\lambda_1[A] \sim L^c$ for the $3d$ SU(2) case (A.C., A. Maas & T. Mendes, 2006). (Similar results in $2d$ and $4d$.)

Convexity of Ω

The gauge condition $\partial \cdot A = 0$ and the operators $D^{bc}(x,y)[A]$, $\mathcal{M}(b,x;c,y)[A] = -\partial^2 + \mathcal{K}[A]$ and $\mathcal{K}[A]$ are linear in the gauge field A_μ:

$$\begin{aligned} \mathcal{M}[\gamma A_1 + (1-\gamma)A_2] &= -\partial^2 + \mathcal{K}[\gamma A_1 + (1-\gamma)A_2] \\ &= \gamma\left(-\partial^2 + \mathcal{K}[A_1]\right) + (1-\gamma)\left(-\partial^2 + \mathcal{K}[A_2]\right) \\ &= \gamma\mathcal{M}[A_1] + (1-\gamma)\mathcal{M}[A_2] \end{aligned}$$

and, for $\gamma \in [0,1]$, $\mathcal{M}[\gamma A_1 + (1-\gamma)A_2]$ is semi-positive definite if $\mathcal{M}[A_1]$ and $\mathcal{M}[A_2]$ are semi-positive definite. Also

$$\gamma\,\partial \cdot A_1 + (1-\gamma)\,\partial \cdot A_2 = 0$$

if $\partial \cdot A_1 = \partial \cdot A_2 = 0$. $\Longrightarrow$ The convex combination $\gamma A_1 + (1-\gamma)A_2$ belongs to Ω, for any value of $\gamma \in [0,1]$, if $A_1, A_2 \in \Omega$.

Boundary of Ω

Using properties 1 and 2 and with $A_1 = 0$, $A_2 = A$, $1 - \gamma = \rho$ we have

$$\mathcal{M}[\rho A] = -\partial^2 + \mathcal{K}[\rho A] = (1-\rho)\,(-\partial^2) + \rho\,\mathcal{M}[A]$$

and, if $A \in \Omega$, then $\rho A \in \Omega$ for any value of $\rho \in [0, 1]$.

Since the color indices of $\mathcal{K}[A]$ are given by $\mathcal{K}^{bc}[A] \sim f^{bce} A^e_\mu$, we have that all the diagonal elements of $\mathcal{K}[A]$ are zero $\Longrightarrow$ the trace of the operator $\mathcal{K}[A]$ is zero.

The operator $\mathcal{K}^{bc}_{xy}[A]$ is real and symmetric (under simultaneous interchange of x with y and b with c) and its eigenvalues are real $\Longrightarrow$ at least one of the eigenvalues of $\mathcal{K}[A]$ is (real and) negative. If ϕ_{neg} is the corresponding eigenvector, that for a sufficiently large (but finite) value of $\rho > 1$ the scalar product $(\phi_{neg}, \mathcal{M}[\rho A]\phi_{neg})$ must be negative $\Longrightarrow$ $\mathcal{M}[\rho A]$ is not semi-positive definite and $\rho A \notin \Omega$.

Proof of the Lower Bound for λ_1 (I)

Consider a configuration A' belonging to the boundary $\partial\Omega$ of Ω and write

$$\lambda_1 \left[\mathcal{M}[\rho A'] \right] = \lambda_1 \left[(1-\rho)\,(-\partial^2) + \rho\,\mathcal{M}[A'] \right] \; .$$

From the second property, $\rho A' \in \Omega$ for $\rho \in [0,1]$. Since

$$\lambda_1 \left[(1-\rho)\,(-\partial^2) + \rho\,\mathcal{M}[A'] \right]$$

$$= \min_{\chi} \left(\chi \, , \left[\, (1-\rho)\,(-\partial^2) + \rho\,\mathcal{M}[A'] \, \right] \, \chi \right) \; ,$$

with $(\chi \, , \chi) = 1$ and $\chi \neq$ constant, we can use the concavity of the minimum function

$$\boxed{\min_{\chi} \left(\chi, [M_1 + M_2]\, \chi \right) \, \geq \, \min_{\chi} \left(\chi, M_1 \chi \right) + \min_{\chi} \left(\chi, M_2 \chi \right) \, .}$$

Proof of the Lower Bound for λ_1 (II)

We find

$$\lambda_1 \left[\mathcal{M}[\rho A'] \right] \,=\, \lambda_1 \left[(1-\rho)\,(-\partial^2) \,+\, \rho\, \mathcal{M}[A'] \right]$$

$$\geq (1-\rho) \min_{\chi} \left(\chi, (-\partial^2)\, \chi \right) \,+\, \rho \min_{\chi} \left(\chi \,, \mathcal{M}[A']\, \chi \right)$$

$$=\, (1-\rho)\, p_{min}^2 \,.$$

Recall that $A' \in \partial\Omega \Longrightarrow$ the smallest non-trivial eigenvalue of the FP matrix $\mathcal{M}[A']$ is null, and that the smallest non-trivial eigenvalue of (minus) the Laplacian $-\partial^2$ is p_{min}^2.

With $\rho A' = A$ the above inequality may also be written as

$$\lambda_1 \left[\mathcal{M}[A] \right] \,\geq\, \left[1 - \rho(A) \right] p_{min}^2 \,.$$

Crossing the Horizon (I)

N	$\max(n)$	$\min(n)$	$\langle n \rangle$	R_{before}	R_{after}
16	30	6	17.2	15(3)	-30(12)
24	27	4	15.1	20(7)	-26(6)
32	19	5	11.7	26(9)	-51(20)
40	18	4	9.4	155(143)	-21(6)
48	13	2	7.8	21(5)	-21(5)
56	12	3	7.6	16(4)	-21(7)
64	11	2	6.8	20(7)	-42(18)
72	11	2	6.1	129(96)	-42(13)
80	12	3	6.1	15(4)	-24(4)

The maximum, minimum and average number of steps n, necessary to "cross the Gribov horizon" along the direction $A^b_\mu(x)$, as a function of the lattice size N. We also show the ratio $R[A] = (S''')^2/(S''\, S'''')$, divided by 1000, for the modified gauge fields $\tau_{n-1} A^b_\mu(x)$ and $\tau_n A^b_\mu(x)$, i.e. for the configurations immediately before and after crossing $\partial\Omega$.

Crossing the Horizon (II)

The case of a typical configuration.

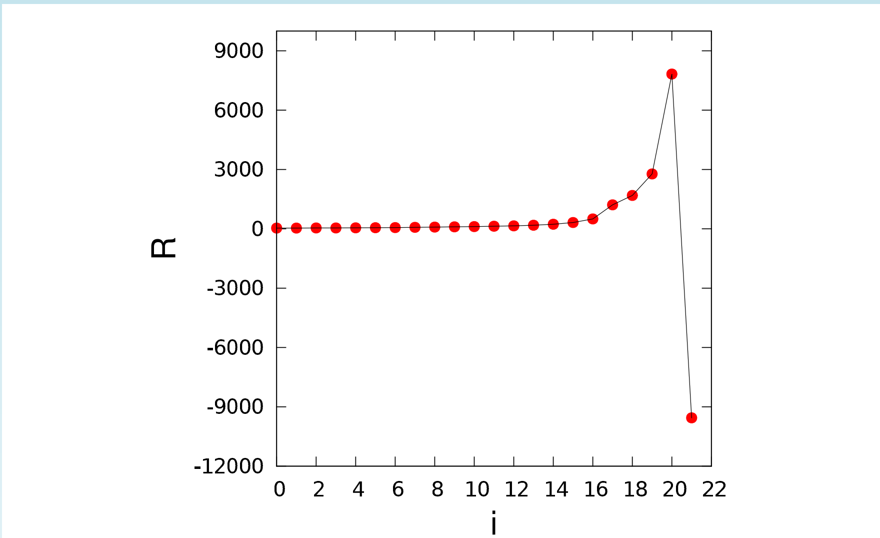

Plot of the ratio R, as a function of the iteration step i, for a configuration with lattice volume 16^4.

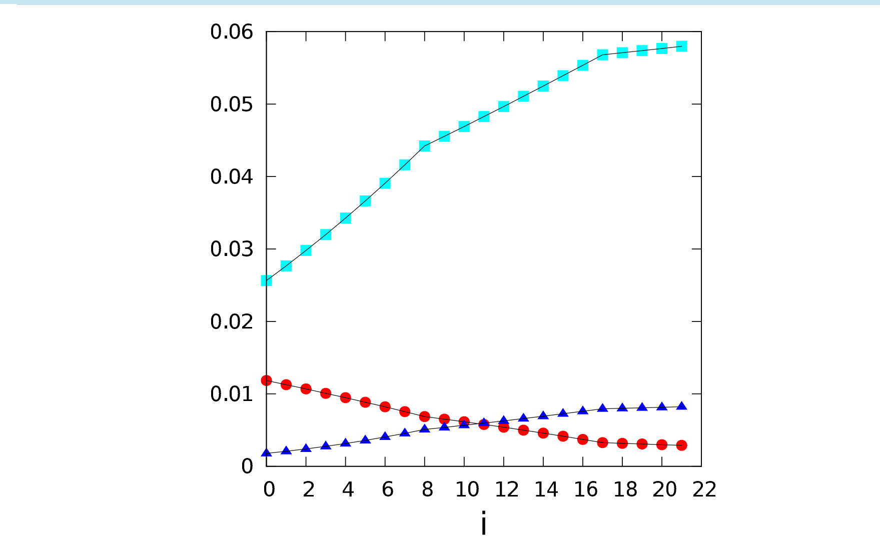

Plot of λ_2 (full circes), $|\mathcal{E}'''|$ (full squares) and $\mathcal{E}''''$ (full triangles) as a function of the iteration step i, for the same configuration.

Crossing the Horizon (III)

The case $R \approx 0$ (configuration on $\partial\Omega \cap \partial\Lambda$).

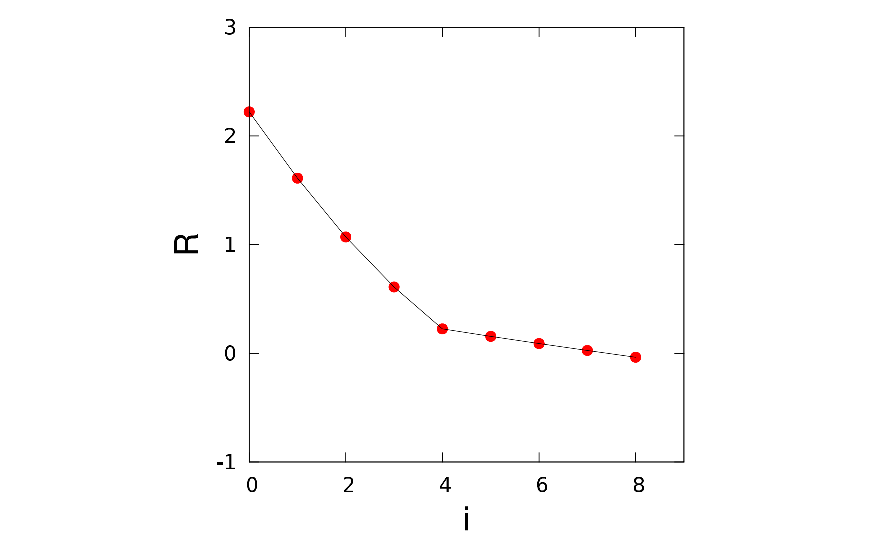

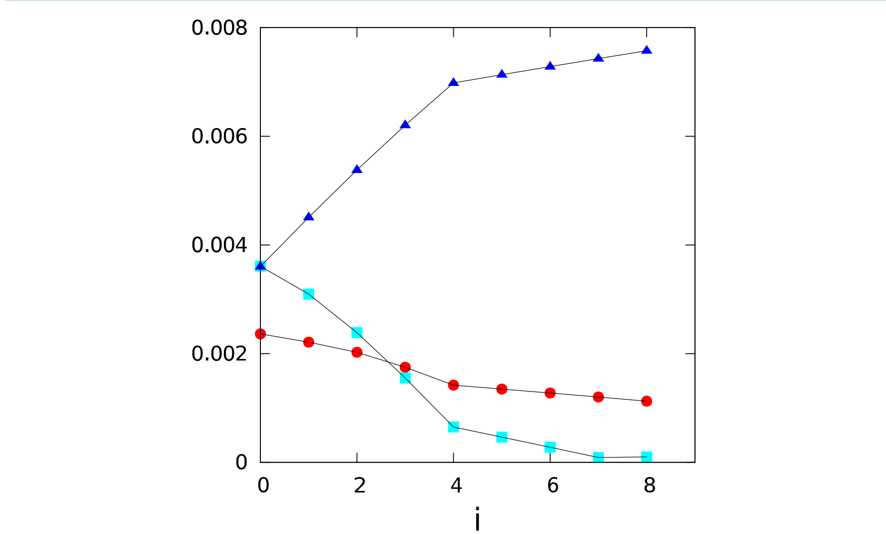

Plot of the ratio R, as a function of the iteration step i, for a configuration with lattice volume 48^4.

Plot of λ_2 (full circes), $|\mathcal{E}'''|$ (full squares) and $\mathcal{E}''''$ (full triangles) as a function of the iteration step i, for the same configuration.